Journal of Materials Chemistry A

PAPER

View Article Online
View Journal | View Issue



Cite this: J. Mater. Chem. A, 2014, 2, 770

# Facile preparation of a nanostructured functionalized catalytically active organosalt†

Ahmad Reza Moosavi-Zare,*[a] Mohammad Ali Zolfigol,*[b] Vahid Khakyzadeh,[b] Christoph Böttcher,[c] Mohammad Hassan Beyzavi,[d] Abdolkarim Zare,[e] Alireza Hasaninejad[f] and Rafael Luque[g]

Received 2nd September 2013
Accepted 29th October 2013

DOI: 10.1039/c3ta13484a

www.rsc.org/MaterialsA

We report a novel nanostructured organosalt, based on sulfonic acid functionalized pyrazinium {[H-pyrazine–$SO_3H$]$Cl_2$} that was synthesized and characterized by several techniques including Fourier transform infrared (FT-IR) spectroscopy, X-ray diffraction (XRD), thermal gravimetric analysis (TGA), differential thermal gravimetric (DTG) analysis, transmission electron microscopy (TEM), mass spectrometry (MS), proton NMR ($^1$H NMR), carbon-13 NMR ($^{13}$C NMR) and also electron diffraction (ED) patterns. Results proved that the unprecedented sulfonated pyrizinium organosalt is indeed nanostructured and highly crystalline as supported by TEM, ED and XRD studies, having an average nanoparticle size of 50 nm according to TEM micrographs. The novel nano-organocatalyst was proved to be an efficient catalyst in the synthesis of 1,2,4,5-tetrasubstituted imidazoles by a one-pot multi-component condensation of benzil, a broad range of aldehydes, primary amines and ammonium acetate at 90 °C under solvent-free conditions.

## Introduction

The design and application of high performance catalysts in synthetic organic protocols including metal-free organic molecules (organocatalysts) and organometallic catalysts have attracted a significant amount of interest from the scientific community in order to develop increasingly attractive methodologies for the preparation of more complex molecules.[1] Organocatalysts have a significant impact and direct benefit in the production of pharmaceutical intermediates when compared with (transition) metal catalysts.

In addition, organocatalysts are commonly inexpensive, stable and readily available, show low toxicity and no sensitivity towards moisture or oxygen.[2] Another advantage of organocatalysts relates to their favourable surface to volume ratio which enhances the contact between reactants and catalyst support and in turn increases the catalytic activity.[3] In spite of their controversy as greener compounds, ionic liquids (ILs) can be considered as organocatalysts.[4] In this context, we have recently reported a novel family of ionic liquids based on acidic sulfonic acid functionalized imidazolium salts (SAFIS).[5–14] S–N bond formation yielding imidazole derivatives as a five member heterocyclic ring compound was reported for the first time by employing such acidic ILs as catalysts. Importantly, the catalytic activities of these acidic-functionalized organocatalysts were further extended to chemistries involving the preparation of bis(indolyl)methanes,[5] *N*-sulfonyl imines,[6] nitro aromatic compounds,[7,8] 1-amidoalkyl-2-naphthols,[9] xanthenes,[10] 1-carbamatoalkyl-2-naphthols,[11] 4,4′-(arylmethylene)-bis(3-methyl-1-phenyl-1*H*-pyrazol-5-ol)s,[12] *tert*-butyl aryl carbamates[13] and hexahydroquinolines.[14]

In continuation of previous research endeavours related to the design and development of novel acidic functionalised ILs and solid salts for organic transformations, we have now prepared and characterized a novel nanostructured organosalt (sulfonic acid pyrazinium chloride) (Scheme 1). The synthesized organocatalyst was successfully employed in the synthesis of different poly-substituted imidazole derivatives exhibiting various important properties (Scheme 2).

Imidazoles are one of the most important groups of five membered nitrogen heterocycles which have attracted much attention because of their participation in the structure and activity of biological molecules including histidine, histamine or biotin.[15] Importantly, there is high demand for these

[a]Department of Chemistry, University of Sayyed Jamaleddin Asadabadi, Asadabad, 6541835583, Iran. E-mail: moosavizare@yahoo.com; Fax: +98 81 23237450

[b]Faculty of Chemistry, Bu-Ali Sina University, Hamedan, 6517838683, Iran. E-mail: mzolfigol@yahoo.com; mr.khakyzadeh@yahoo.com

[c]Research Center of Electron Microscopy, Institute for Chemistry and Biochemistry, Freie Universität Berlin, Fabeckstraße 36a, 14195 Berlin, Germany

[d]Institut für Chemie und Biochemie, Freie Universität Berlin, Takustr. 3, 14195 Berlin, Germany

[e]Department of Chemistry, Payame Noor University, 19395-4697 Tehran, Iran

[f]Department of Chemistry, Faculty of Sciences, Persian Gulf University, Bushehr 75169, Iran

[g]Departamento de Quimica Organica, Universidad de Córdoba, Edif. Marie Curie, Ctra Nnal IV-A Km 396, E14014, Córdoba, Spain. E-mail: q62alsor@uco.es

† Electronic supplementary information (ESI) available. See DOI: 10.1039/c3ta13484a

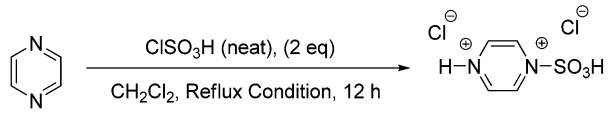


Scheme 1 The preparation of sulfonic acid functionalized pyrazinium salt {[H-pyrazine–$SO_3H$]$Cl_2$}.

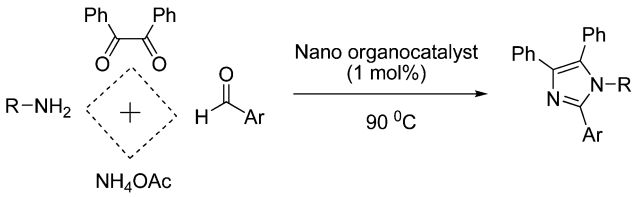


Scheme 2 The preparation of 1,2,4,5-tetrasubstituted imidazoles (R and Ar groups are given in Table 1).

compounds from the pharmaceutical viewpoint and the imidazole moiety is the core structure of important drugs such as losartan, olmesartan, eprosartan and trifenagrel (Fig. 1).[16]

Moreover, they are very popular as ILs[17] and *N*-heterocyclic carbenes (NHCs) in organometallic chemistry have been increased.[18,19]

Several catalytic methods have been reported to improve the yields for the synthesis of polysubstituted imidazoles. Catalysts employed in this process include heteropolyacids,[20] silica gel and zeolites,[21] alumina,[22] $HClO_4$–$SiO_2$,[23] $I_2$,[24] $BF_3 \cdot SiO_2$,[25] $InCl_3 \cdot 3H_2O$,[26] $K_5CoW_{12}O_{40} \cdot 3H_2O$,[27] copper acetate,[28] or trifluoroacetic acid using microwave irradiation.[29] Other examples for the synthesis of polysubstituted imidazoles have also been reported in the literature.[30]

However, most of the reported protocols have inherent drawbacks related to laborious and complex reaction workup, tedious purification steps, generation of significant amounts of waste, employment of strongly acidic conditions, side reactions, poor yields and the use of expensive or sophisticated catalysts. Comparatively, the utilization of the proposed organosalt as a catalyst in the synthesis of substituted imidazoles can provide additional advantages in terms of reaction efficiency, selectivity and the possibility of recycling the catalyst for further use. To the best of our knowledge, this is also the first report of the preparation of a catalytically active nanostructured organosalt.

## Results and discussion

The expected di-sulfonic acid functionalized pyrazinium salt {*i.e.* [$SO_3$–pyrazine–$SO_3H$]$Cl_2$} was surprisingly not observed in the synthesis of the sulfonic acid functionalized pyrazinium salt, with mono-functionalized [H-pyrazine–$SO_3H$]$Cl_2$ as the main product (Scheme 3).

Characterization of {[H-pyrazine–$SO_3H$]$Cl_2$} was carried out using various analytical techniques including IR, $^1$H NMR, $^{13}$C NMR and mass spectrometry.

The IR spectrum of the catalyst showed a broad peak at 2650–3500 $cm^{-1}$ which could contain the overlaid $NH^+Cl^-$ stretching peak (2800 $cm^{-1}$, bs),[31] and the O–H stretching of $SO_3H$. Moreover, the two peaks observed at 1069 $cm^{-1}$ and 1174 $cm^{-1}$ correspond to vibrational modes of N–$SO_2$ and O–$SO_2$ bonds. Another peak at 1010 could be correlated with S=O bonds (Fig. 2).

The important peak found in $^1$H NMR spectra of the catalyst is related to the acidic hydrogen of $SO_3H$ which was observed at 13.23 ppm (Fig. 3b). $^1$H NMR spectra of $ClSO_3H$ (starting material) as well as [H-pyrazine–H]$Cl_2$ in DMSO {[H-pyrazine–H][$ClSO_3$]$_2$ was not commercially available and [H-pyrazine–H]$Cl_2$ has the same type of acidic H environments} were run to further confirm the presence of $SO_3H$ hydrogen in the catalyst (and not to unreacted starting material or possible byproducts).

In these spectra, the peaks of the acidic hydrogens of [H-pyrazine–$SO_3H$]$Cl_2$, $ClSO_3H$ and [H-pyrazine–H]$Cl_2$ were observed at 13.23, 10.75 and 9.25 ppm, respectively (Fig. 3a).

The difference between the peaks of the acidic hydrogens in the compounds confirmed that the peak observed at 13.23

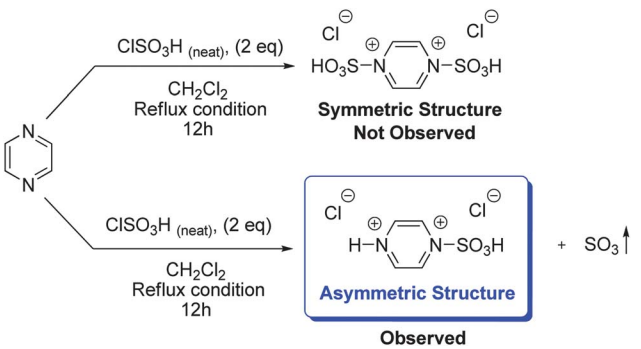


Scheme 3 The preparation of sulfonic acid functionalized pyrazinium salt {[H-pyrazine–$SO_3H$]$Cl_2$}.

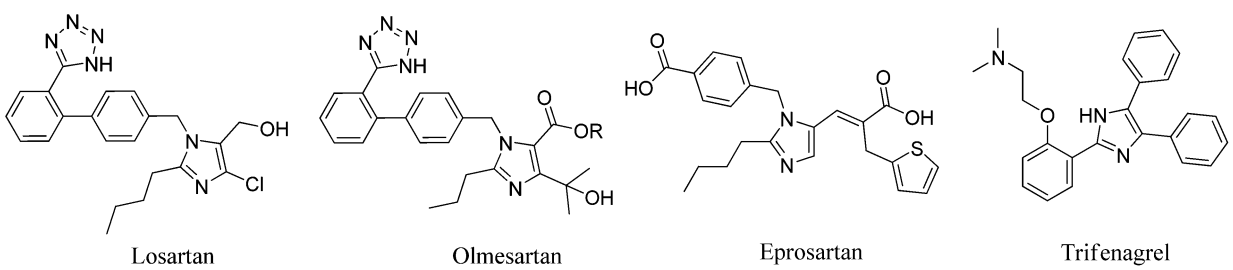


Fig. 1 The structure of a few exemplary drugs such as losartan, olmesartan, eprosartan and trifenagrel, which incorporate an imidazole moiety.

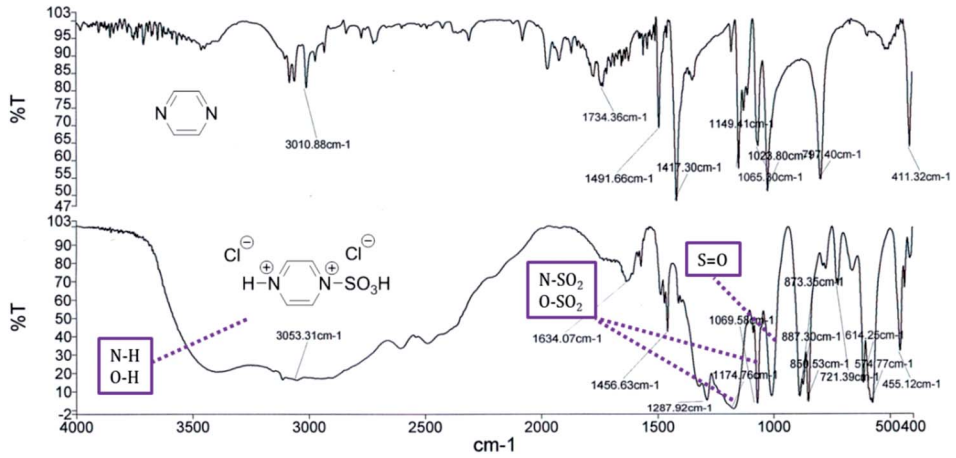


Fig. 2 IR spectrum of sulfonic acid functionalized pyrazinium salt {[H-pyrazine–$SO_3H$]$Cl_2$}.

ppm of the $^1$H NMR spectra of [H-pyrazine–$SO_3H$]$Cl_2$ is correctly related to the hydrogen of the $SO_3H$-functionalized pyrazinium salt.

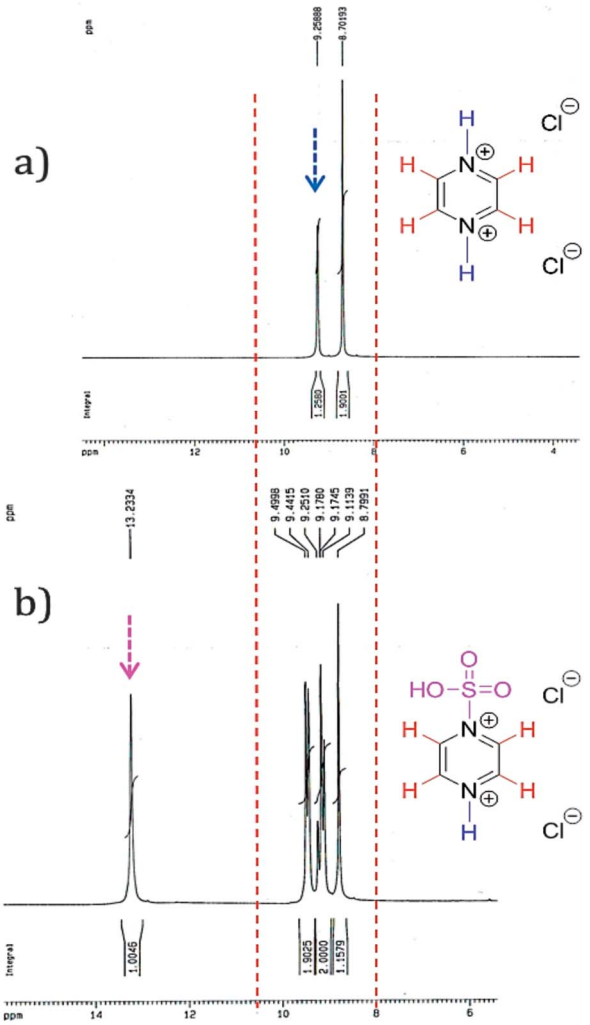


Fig. 3 (a) $^1$H NMR spectra of pyrazinium chloride {[H-pyrazine–H]$Cl_2$}; (b) $^1$H NMR spectra of sulfonic acid functionalized pyrazinium salt {[H-pyrazine–$SO_3H$]$Cl_2$}.

Results were also in good agreement with mass spectra of [H-pyrazine–$SO_3H$]$Cl_2$, which indicated a parent peak of 233 *m*/*z*, the expected mass of the catalyst (ESI†).

Another set of evidence of the structure of the catalyst was obtained from $^{13}$C NMR spectra. Two peaks present at 144.26 and 150.75 support the proposed asymmetric structure of the catalyst from Scheme 3 (Fig. 4).

XRD patterns of the catalyst {[H-pyrazine–$SO_3H$]$Cl_2$} were investigated in a domain of 10–90 degrees (Fig. 5). As shown in Fig. 5, the patterns exhibited diffraction lines of a highly crystalline structure at $2\theta \approx 14.48°$, 16.97°, 18.50°, 18.80°, 19.09°, 22.38°, 25.08°, 26.03°, 27.86°, and 28.45°, and several small lines in the 30–60° range. Peak width (FWHM), size and inter-planar distance studies of the catalyst could be worked out in the 14.5 to 33. 3 degree range and the results are summarized in Table 1. As an example, calculations for the highest diffraction line 26.03° proved that an FWHM of 0.126, a crystallite size of *ca.* 120 nm, calculated *via* the Scherrer

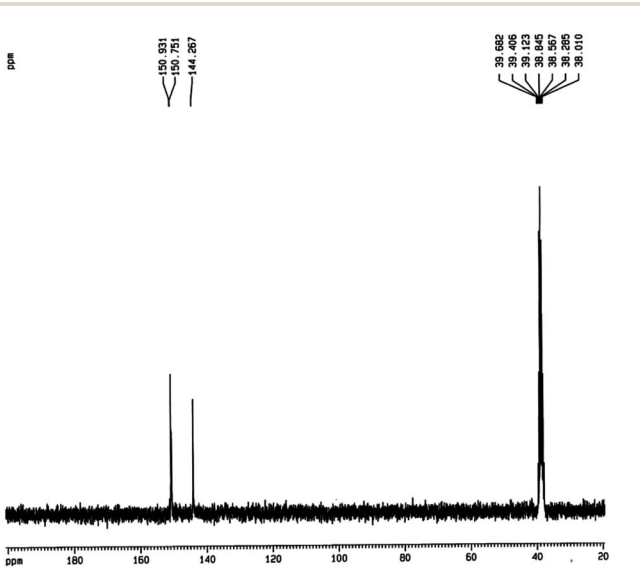


Fig. 4 $^{13}$C NMR spectra of sulfonic acid functionalized pyrazolium salt {[H-pyrazine–$SO_3H$]$Cl_2$}.

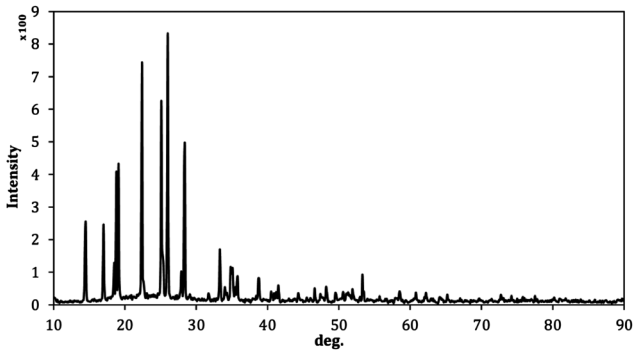


Fig. 5 XRD pattern of the nanostructured organosalt.

Table 1 XRD data for the catalyst {[H-pyrazine–$SO_3H$]$Cl_2$}

| Entry | 2$\theta$ | Peak width [FWHM] | Size [nm] | Inter planer distance [nm] |
|---|---|---|---|---|
| 1 | 14.50 | 0.212 | 54 | 0.610853 |
| 2 | 16.99 | 0.163 | 77 | 0.521848 |
| 3 | 18.79 | 0.258 | 43 | 0.472243 |
| 4 | 19.10 | 0.198 | 60 | 0.464649 |
| 5 | 22.41 | 0.146 | 93 | 0.396712 |
| 6 | 25.10 | 0.108 | 157 | 0.354771 |
| 7 | 26.01 | 0.126 | 119 | 0.342563 |
| 8 | 28.30 | 0.184 | 69 | 0.315343 |
| 9 | 33.30 | 0.152 | 93 | 0.269048 |

equation [$D = K\lambda/(\beta \cos \theta)$], and an inter-planar distance of 0.343 nm (calculated using the Bragg equation: $d_{hkl} = \lambda/(2 \sin \theta)$, $\lambda$: Cu radiation (0.154178 nm)) were obtained. Most importantly, crystallite sizes as obtained from the various diffraction lines using the Scherrer equation were found to be in the nanometer range (50–160 nm), a most relevant finding for the synthesized organosalt.

To further confirm the nanostructure of the synthesized organosalt, TEM measurements were performed as depicted in Fig. 6a.

The TEM micrograph (Fig. 6a) confirmed the presence of more or less spherical nanoparticles with a mean diameter of 51 nm (Fig. 6b, from the analysis of 307 particles *via* image processing program of Fig. 6a). TEM imaging was complemented by electron diffraction (ED) patterns (Fig. 6c) to check the materials' crystalline nature. The most prominent ED rings corresponded to real spacings at 0.5219 nm, in good agreement with XRD results (Table 1, entry 2). Additional prominent diffraction rings could be observed at 0.438 nm (no analogous value in XRD), 0.397 nm (Table 1, entry 5) and 0.317 nm (Table 1, entry 8). ED results further confirmed the nanoscale nature of the synthesized organosalt.

The stability of the catalyst was further investigated by thermal gravimetric (TG) and differential thermal gravimetric (DTG) analyses. TG and DTG plots in Fig. 7 indicate that weight loss of [H-pyrazine–$SO_3H$]$Cl_2$ occurred in a single step after 280 °C, so that [H-pyrazine–$SO_3H$]$Cl_2$ is in principle stable up to 280 °C. The TG pattern coincides with a single stage decomposition of the organosalt in which no additional intermediate was identified.

Upon detailed characterization and stability studies, [H-pyrazine–$SO_3H$]$Cl_2$ was subsequently investigated as a catalyst for organic transformations.

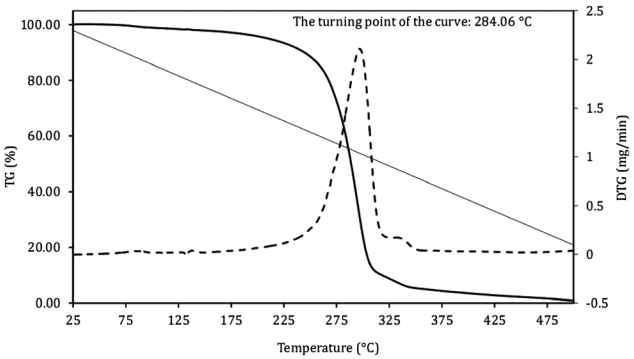


Fig. 7 TG/DTG plots of the [H-pyrazine–$SO_3H$]$Cl_2$.

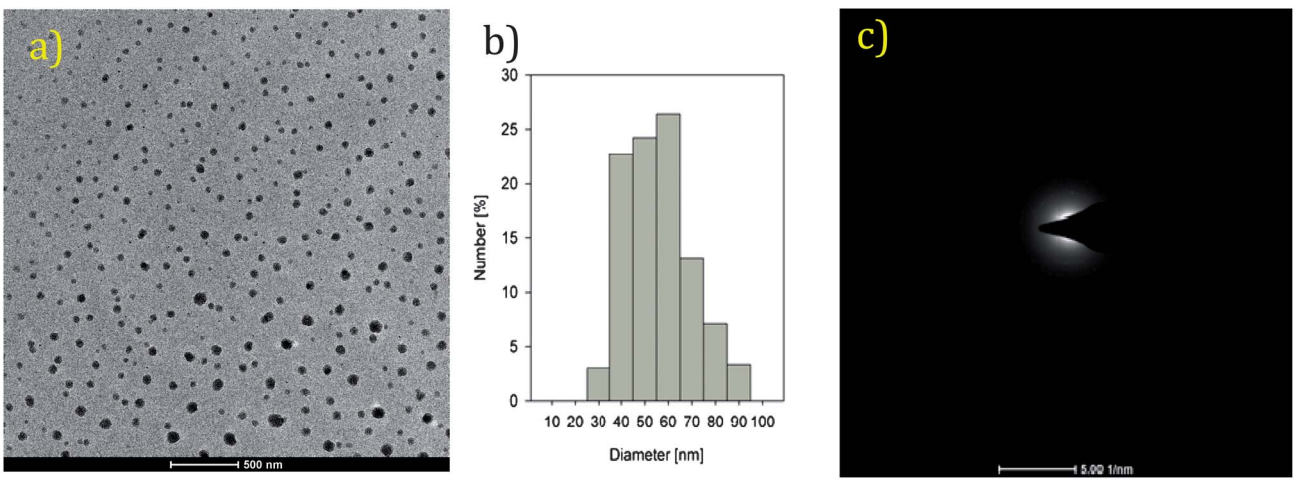


Fig. 6 (a) Transmission electron micrographs (TEM) of the catalyst particles; (b) histogram of the size distribution of 307 catalyst particles taken from (a); (c) electron diffraction (ED) patterns of the catalyst.

The synthesis of polysubstituted imidazoles was selected as the test reaction for the organocatalyst. Preliminary experiments were aimed to screen and optimize reaction conditions for the model reaction of benzil (1 mmol), 4-chlorobenzaldehyde (1 mmol), benzylamine (1 mmol) and ammonium acetate (1 mmol) under mild temperature (80–95 °C). Results summarized in Fig. 8 pointed out that optimum results were obtained using catalytic amounts (1 mol%) [H-pyrazine–$SO_3H$]$Cl_2$ at 90 °C. In principle, this reaction could be then considered as solventless. The use of [H-pyrazine–H]$Cl_2$ as well as $H_2SO_4$ as alternative catalysts in the reaction provided comparably lower yields to the target product under investigated reaction conditions (Fig. 8).

Upon optimization of reaction conditions, the scope and efficiency of the process were subsequently explored for a range of structurally diversed aromatic aldehydes as well as amines (aliphatic or aromatic). Gratifyingly, the proposed reaction catalysed by the nanostructured organosalt was amenable to several susbtrates under very mild reaction conditions and short times of reaction (typically 90 °C, Table 2).

A number of substituted imidazole products could be obtained in good to excellent yields in the absence of byproducts under the investigated conditions.

The proposed catalytic routes are depicted in Scheme 4, which are consistent with literature reports.[14,19,32] The nanoorganosalt [H-pyrazine–$SO_3H$]$Cl_2$ has two acidic hydrogens which can participate in hydrogen bonding. Consequently, both aldehydes and benzil were activated by [H-pyrazine–$SO_3H$]$Cl_2$ to accept nucleophiles. In particular, we believe that the differences in acidity of the $SO_3H$ hydrogen from [H-pyrazine–$SO_3H$]

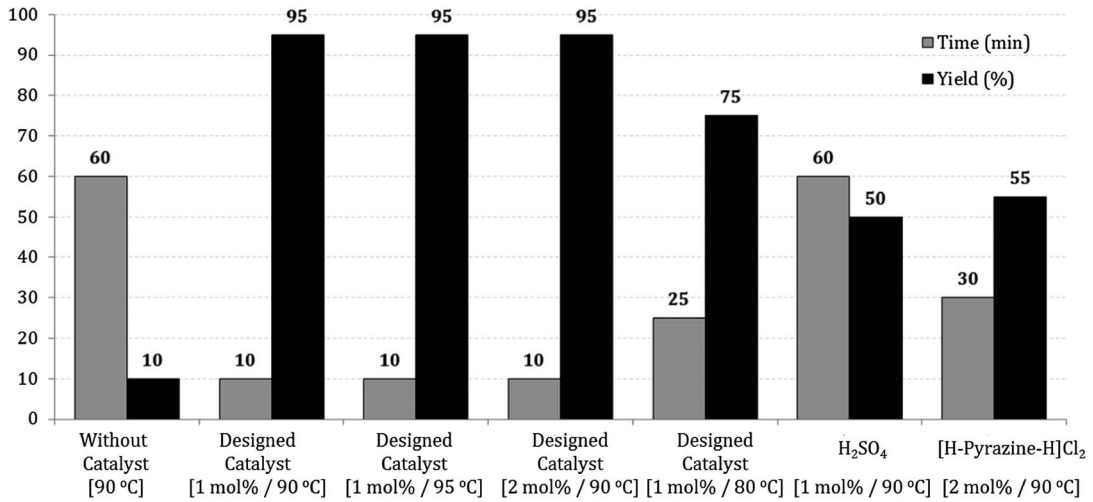


Fig. 8 Effect of different amounts of the catalyst loading and temperature on the reaction of benzil, 4-chlorobenzaldehyde, benzylamine and ammonium acetate.

Table 2 The synthesis of 1,2,4,5-tetrasubstituted imidazoles using [H-pyrazine–$SO_3H$]$Cl_2$ (1 mol%) under solvent-free conditions at 90 °C[a]

| Entry | Ar | R | Time (min) | Yield[b] (%) | Mp (°C) found/(reported) |
|---|---|---|---|---|---|
| **1a** | $C_6H_5$ | $C_6H_5$ | 10 | 86 | 219–220/(218–219)[20] |
| **1b** | $C_6H_5$ | $C_6H_5CH_2$ | 15 | 87 | 155–158/(158–160)[20] |
| **1c** | 4-$CH_3$–$C_6H_4$ | $C_6H_5$ | 25 | 80 | 189–191/(189–190)[20] |
| **1d** | 4-$CH_3$–$C_6H_4$ | $C_6H_5CH_2$ | 15 | 90 | 164–167/(165–166)[20] |
| **1e** | 4-Cl–$C_6H_4$ | 4-Cl–$C_6H_4$ | 10 | 85 | 188–189/(189–191)[18] |
| **1f** | 3-$NO_2$–$C_6H_4$ | 4-$CH_3$–$C_6H_4$ | 25 | 80 | 146–149/(149–151)[18] |
| **1g** | 4-$NO_2$–$C_6H_4$ | 4-$CH_3$–$C_6H_4$ | 15 | 90 | 216–219/(215–217)[18] |
| **1h** | 4-Cl–$C_6H_4$ | $C_6H_5CH_2$ | 10 | 95 | 157–159/(161–163)[18] |
| **1i** | 4-Cl–$C_6H_4$ | 4-F–$C_6H_4$ | 10 | 90 | 195–199/(198–201)[18] |
| **1j** | 4-$CH_3$–$C_6H_4$ | 4-$CH_3$–$C_6H_4$ | 15 | 80 | 190–193/(194–196)[18] |
| **1k** | 3-$OCH_3$–$C_6H_4$ | $C_6H_5CH_2$ | 25 | 80 | 131–132/(128–130)[23] |
| **1l** | 4-Cl–$C_6H_4$ | $C_6H_5$ | 10 | 85 | 147–150/(148–150)[31] |
| **1m** | 4-OH–$C_6H_4$ | $C_6H_5CH_2$ | 20 | 85 | 133–136/(134–135)[23] |
| **1n** | 4-$OCH_3$–$C_6H_4$ | $C_6H_5CH_2$ | 15 | 85 | 155–167/(157–160)[22] |
| **1o** | 4-OH–$C_6H_4$ | $C_6H_5$ | 15 | 92 | 279–282/(280–281)[25] |
| **1p** | 4-CN–$C_6H_4$ | 4-$CH_3$–$C_6H_4$ | 15 | 95 | 197–199/(198–201)[18] |
| **1q** | 3-OH–$C_6H_4$ | 4-$CH_3$–$C_6H_4$ | 15 | 85 | 231–233/(230–232)[27] |
| **1r** | 2-Thienyl | 4-$CH_3$–$C_6H_4$ | 25 | 85 | 198–201/(199–202)[18] |
| **1s** | 2-Thienyl | 4-OH–$C_6H_4$ | 15 | 87 | 199–202/(198–201)[18] |

[a] $^1$H NMR and $^{13}$C NMR of products given in the ESI. [b] Yield of the purified product.

 

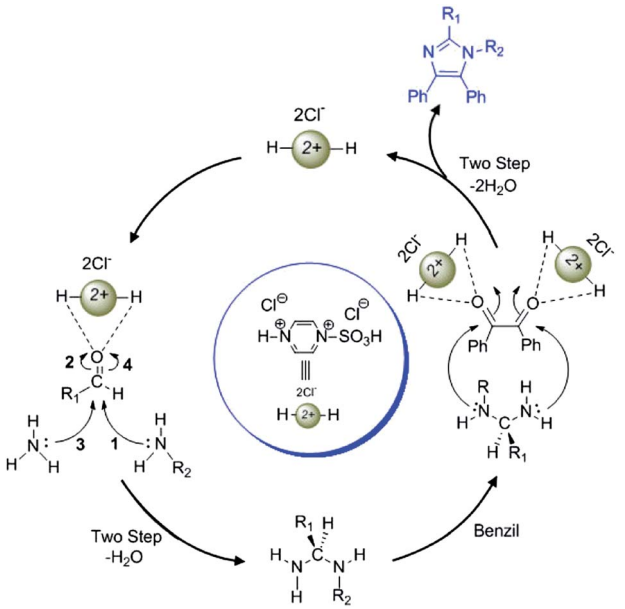


Scheme 4 Proposed reaction mechanism for the synthesis of 1,2,4,5-tetrasubstituted imidazoles using [H-pyrazine–$SO_3H$]$Cl_2$.

$Cl_2$ as compared to those of [H-pyrazine–H]$Cl_2$ and $H_2SO_4$ may account for the observed improved catalytic activity in Fig. 8. A partial contribution of the nanocrystallinity of the organosalt cannot be either ruled out but this (if any) would be in principle expected to be not very significant. Also, the formation of several hydrogen bonds between substrates and catalyst could facilitate a more efficient catalysis in the reaction. High reaction rates could also be influenced by the organosalt nanostructure, which will be investigated in due course.

The recovery and reuse of the catalyst was also examined for the reactions of benzil, 4-chlorobenzaldehyde, benzylamine and ammonium acetate by means of a hot filtration test.[33] The reaction mixture was filtered off half way through reaction, extracted using hot absolute ethanol or ethyl acetate and separated out from the catalyst. The reused catalyst upon filtration was subsequently employed in another reaction run with fresh reagents while the filtrate of the reaction mixture was left reacting for several hours.

The catalytic activity of the nano-organocatalyst was found to be almost preserved after five successive runs, with a slight decrease in rate constant (by a factor of two, assuming a first order kinetics). Nevertheless, products were obtained in excellent yield after five runs in a short time of reaction (typically 10–15 min, Table 3). The analogous reaction from the filtrate did not react further under similar reaction conditions even after 1 h reaction.

Table 3 Reuses of [H-pyrazine–$SO_3H$]$Cl_2$ in the reaction between benzil, 4-chlorobenzaldehyde, benzylamine and ammonium acetate at 90 °C

| Run | 1 | 2 | 3 | 4 | 5 |
|---|---|---|---|---|---|
| Time [min] | 10 | 10 | 12 | 13 | 15 |
| Yield[a] [%] | 95 | 93 | 93 | 91 | 90 |

[a] Isolated yield.

## Conclusions

A novel nanostructured sulfonic acid functionalized pyrazinium salt {[H-pyrazine–$SO_3H$]$Cl_2$} was synthesized, characterized and tested as a reusable nano-organosalt in the one-pot four-component reaction of aldehydes (hetero-aromatic and aromatic aldehydes), amines (aliphatic or aromatic), benzil and ammonium acetate under mild reaction conditions to give 1,2,4,5-tetrasubstituted imidazoles. Excellent features of the proposed methodology include high efficiency, versatility, short times of reaction, high yields to products, cleaner reaction profiles and simplicity, making it an attractive alternative for the clean synthesis of substituted imidazoles as biologically and pharmaceutically relevant materials.

## Experimental section

### Materials

All chemicals were purchased from Merck or Fluka Chemical Companies. Known products were identified by comparison of their melting points and spectral data with those in the authentic samples. $^1$H NMR (500 MHz) and $^{13}$C NMR (125 MHz) were run on a Bruker Avance DPX-250 FT-NMR spectrometer ($\delta$ in ppm). Melting points were recorded on a Büchi B-545 apparatus in open capillary tubes. The crystal structure of synthesized materials was determined using an X-ray diffractometer (Italstructure ADP2000 XRD) at ambient temperature. Mass spectra were recorded on a Shimadzu GC MS-QP 1000 EX 85 apparatus. Thermal gravimetry (TG) and differential thermal 88 gravimetric (DTG) analysis were performed on a Perkin Elmer Model: 89 Pyris 1. Transmission electron microscopy imaging was carried out using a Tecnai F20 (FEI company, Oregon, USA) with field emission illumination operated at an acceleration voltage of 160 kV.

### Procedure for the preparation of sulfonic acid functionalized pyrazinium salt {[H-pyrazine–$SO_3H$]$Cl_2$} (Scheme 3)

Chlorosulfonic acid (1.177 g, 10.2 mmol) was added dropwise into a round-bottomed flask (50 mL) containing pyrazine (0.400 g, 5 mmol) in $CH_2Cl_2$ (20 mL) over a period of 30 min at room temperature. Upon complete addition, the reaction mixture was stirred and heated under reflux conditions for 12 h. Upon cooling down very slowly to room temperature, $CH_2Cl_2$ was decanted. The solid residue was then washed with dry $CH_2Cl_2$ (3 × 20 mL) and dried under vacuum to give [H-pyrazine–$SO_3H$]$Cl_2$ as gray solid powder in 98% yield, 1.14 g.

### Procedure for the synthesis of 1,2,4,5-tetrasubstituted imidazoles using [H-pyrazine–$SO_3H$]$Cl_2$ as catalyst (1a–s)

A mixture of benzil (1 mmol), aldehyde (1 mmol), primary amine (1 mmol), ammonium acetate (1 mmol, as precursor for the *in situ* generation of ammonia) and [H-pyrazine–$SO_3H$]$Cl_2$

(1 mol%) in a 10 mL round-bottomed flask connected to a reflux condenser was stirred in an oil-bath at 90 °C. After completion of the reaction, as monitored by TLC, the mixture was cooled to room temperature. Crude products were dissolved in warm ethanol or warm ethyl acetate and separated off from the catalyst, which was then filtered off. The remaining solid was washed with ethyl acetate (5 mL) and dried under reduced pressure ([H-pyrazine–$SO_3H$]$Cl_2$ was recovered in 95% yield). Then, the pure product was obtained by the recrystallization of the reaction mixture in ethanol or ethyl acetate.

### Characterization methods

Due to the radiation sensitivity of the organic material, the diffraction spacings quickly faded upon irradiation. Low-dose techniques implemented in the microscopes' software were therefore used in order to allow for imaging of the diffraction data.

Thermal gravimetric analysis (TGA) of the sulfonic acid functionalized pyrazinium salt was also studied in a range of 25 up to 800 °C, with a temperature increase rate of 10 °C $min^{-1}$ in a nitrogen atmosphere (Fig. 8).

Samples for TEM were generally prepared by ultrasonication of 10 mg solid in hexane for 30 minutes, which gave a turbid suspension in all cases. The solid was treated beforehand in an agate mortar for milling larger particles. Droplets of the suspension were applied to carbon foil covered microscopical 400 mesh copper grids (BAL-TEC GmbH, Witten, Germany) and dried in air. No additional staining materials were used. The grids were consecutively transferred into a Tecnai F20 FEG transmission electron microscope (FEI company, Oregon, USA) operating at 160 kV acceleration voltage. Images were taken at various magnifications ranging from 2k up to 19k. Data were recorded by the use of an Eagle 2k CCD camera (FEI company) at full resolution (binning 1). The application of the microscopes' low dose routine was necessary for image and diffraction pattern recordings as the crystal ultrastructure turned out to suffer from radiation damage. Diffraction patterns were recorded at a camera length of 520 mm. Calibration was done using a thallium chloride standard (Plano GmbH, Wetzlar, Germany).

## Acknowledgements

The authors gratefully acknowledge partial support of this work by the Research Affairs Office of Bu-Ali Sina University (Grant number 32-1716 entitled development of chemical methods, reagents and molecules), and the Center of Excellence in Development of Chemical Method (CEDCM), Hamedan, I.R. Iran. Rafael Luque gratefully acknowledges MICINN for the concession of a Ramon y Cajal Contract (ref. RYC-2009-04199) and funding from projects CTQ2011-28954-C02-02 (MEC) and P10-FQM-6711 (Consejeria de Ciencia e Innovacion, Junta de Andalucia).

## Notes and references

1 Y. Yu-Dong, Lu. Xu, T. Etsuko and S. Norio, *J. Fluorine Chem.*, 2012, **143**, 204–209.
2 (*a*) P. C. B. Page, M. M. Farah, B. R. Buckley and A. J. Blacker, *J. Org. Chem.*, 2007, **72**, 4424–4430; (*b*) J. Marco-Martínez, V. Marcos, S. Reboredo, S. Filippone and N. Martín, *Angew. Chem., Int. Ed.*, 2013, **52**, 5115–5119; (*c*) R. Gramage-Doria and J. N. H. Reek, *ChemCatChem*, 2013, **5**, 677–679; (*d*) C. Gomez, J.-F. Betzer, A. Voituriez and A. Marinetti, *ChemCatChem*, 2013, **5**, 1055–1065; (*e*) C.-C. Hsiao, H.-H. Liao, E. Sugiono, I. Atodiresei and M. Rueping, *Chem.–Eur. J.*, 2013, **19**, 9775–9779; (*f*) J. Alemán and S. Cabrera, *Chem. Soc. Rev.*, 2013, **42**, 774–793; (*g*) Z. Du and Z. Shao, *Chem. Soc. Rev.*, 2013, **42**, 1337–1378; (*h*) Q. Dai, H. Arman and J. C.-G. Zhao, *Chem.–Eur. J.*, 2013, **19**, 1666–1671; (*i*) B. Bradshaw, C. Luque-Corredera and J. Bonjoch, *Org. Lett.*, 2013, **15**, 326–329; (*j*) E. Mayans, A. Gargallo, Á. Álvarez-Larena, O. Illa and R. M. Ortuño, *Eur. J. Org. Chem.*, 2013, 1425–1433; (*k*) Y. Sohtome, T. Yamaguchi, S. Tanaka and K. Nagasawa, *Org. Biomol. Chem.*, 2013, **11**, 2780–2786.
3 V. Polshettiwar and R. S. Varma, *Green Chem.*, 2010, **12**, 743–754.
4 J. P. Hallett and T. Welton, *Chem. Rev.*, 2011, **111**, 3508–3576.
5 M. A. Zolfigol, A. Khazaei, A. R. Moosavi-Zare and A. Zare, *Org. Prep. Proced. Int.*, 2010, **42**, 95–102.
6 M. A. Zolfigol, A. Khazaei, A. R. Moosavi-Zare and A. Zare, *J. Iran. Chem. Soc.*, 2010, **7**, 646–651.
7 A. Khazaei, M. A. Zolfigol, A. R. Moosavi-Zare and A. Zare, *Sci. Iran., Trans. C*, 2010, **17**, 31–36.
8 M. A. Zolfigol, A. Khazaei, A. R. Moosavi-Zare, A. Zare, H. G. Kruger, Z. Asgari, V. Khakyzadeh and M. Kazem-Rostami, *J. Org. Chem.*, 2012, **77**, 3640–3645.
9 M. A. Zolfigol, A. Khazaei, A. R. Moosavi-Zare, A. Zare and V. Khakyzadeh, *Appl. Catal., A*, 2011, **400**, 70–81.
10 M. A. Zolfigol, V. Khakyzadeh, A. R. Moosavi-Zare, A. Zare, S. B. Azimi, Z. Asgari and A. Hasaninejad, *C. R. Chim.*, 2012, **15**, 719–736.
11 A. Zare, T. Yousofia and A. R. Moosavi-Zare, *RSC Adv.*, 2012, **2**, 7988–7991.
12 A. Khazaei, M. A. Zolfigol, A. R. Moosavi-Zare, Z. Asgari, M. Shekouhy, A. Zare and A. Hasaninejad, *RSC Adv.*, 2012, **2**, 8010–8013.
13 M. A. Zolfigol, V. Khakyzadeh, A. R. Moosavi-Zare, G. Chehardoli, F. Derakhshan-Panah, A. Zare and O. Khaledian, *Sci. Iran., Trans. C*, 2012, **19**, 1584–1590.
14 A. Zare, F. Abi, A. R. Moosavi-Zare, M. H. Beyzavi and M. A. Zolfigol, *J. Mol. Liq.*, 2013, **178**, 113–121.
15 S. A. Laufer, W. Zimmermann and K. J. Ruff, *J. Med. Chem.*, 2004, **47**, 6311–6325.
16 C. Leister, Y. Wang, Z. Zhao and C. W. Lindsley, *Org. Lett.*, 2004, **6**, 1453–1456.
17 P. Wasserscheid and T. Welton, *Ionic Liquids in Synthesis*, Wiley-VCH, Weinheim, 2008.
18 L. H. Lee, M. Bang and C. S. Pak, *Tetrahedron Lett.*, 2005, **46**, 7139–7142.
19 A. Hasaninejad, A. Zare, M. Shekouhi and J. Ameri Rad, *J. Comb. Chem.*, 2010, **12**, 844.
20 M. M. Heravi, F. Derikvand and F. F. Bamoharram, *J. Mol. Catal. A: Chem.*, 2007, **263**, 112–114.

 

21 S. Balalaie and A. Arabanian, *Green Chem.*, 2000, **2**, 274–276.
22 A. Y. Usyatinsky and Y. L. Khmelnitsky, *Tetrahedron Lett.*, 2000, **41**, 5031–5034.
23 S. Kantevari, S. V. N. Vuppalapati, D. O. Biradar and L. Nagarapu, *J. Mol. Catal. A: Chem.*, 2007, **266**, 109–113.
24 M. Kidwai, P. Mothsra, V. Bansal, R. K. Somvanshi, A. S. Ethayathulla, S. Dey and T. P. Singh, *J. Mol. Catal. A: Chem.*, 2007, **265**, 177–179.
25 B. Sadeghi, B. B. F. Mirjalili and M. M. Hashemi, *Tetrahedron Lett.*, 2008, **49**, 2575–2577.
26 S. D. Sharma, P. Hazarika and D. Konwar, *Tetrahedron Lett.*, 2008, **49**, 2216–2220.
27 L. Nagarapu, S. Apuri and S. Kantevari, *J. Mol. Catal. A: Chem.*, 2007, **266**, 104–108.
28 B. H. Lipshutz and M. C. Morey, *J. Org. Chem.*, 1983, **48**, 3745–3750.
29 M. R. Mohammadizadeh, A. Hasaninejad and M. Bahramzadeh, *Synth. Commun.*, 2009, **39**, 3232–3242.
30 (*a*) H. Huang, X. Ji, W. Wu and H. Jiang, *Adv. Synth. Catal.*, 2013, **355**, 170–180; (*b*) Z. Jiang, P. Lu and Y. Wang, *Org. Lett.*, 2012, **14**, 6266–6269; (*c*) B. Hu, Z. Wang, N. Ai, J. Zheng, X.-H. Liu, S. Shan and Z. Wang, *Org. Lett.*, 2011, **13**, 6362–6365; (*d*) Y.-B. Nie, L. Wang and M.-W. Ding, *J. Org. Chem.*, 2012, **77**, 696–700; (*e*) D. Kumar, D. N. Kommi, N. Bollineni, A. R. Patel and A. K. Chakraborti, *Green Chem.*, 2012, **14**, 2038–2049; (*f*) C. Kison and T. Opatz, *Chem.–Eur. J.*, 2009, **15**, 843–845; (*g*) W. Li and Y. Lam, *J. Comb. Chem.*, 2005, **7**, 644–647; (*h*) A. R. Karimi, Z. Alimohammadi, J. Azizian, A. A. Mohammadi and M. R. Mohammadizadeh, *Catal. Commun.*, 2006, **7**, 728–732; (*i*) K. Niknam, A. Deris, F. Naeimi and F. Majleci, *Tetrahedron Lett.*, 2011, **52**, 4642–4645; (*j*) S. Samai, G. C. Nandi, P. Singh and M. S. Singh, *Tetrahedron*, 2009, **65**, 10155–10161; (*k*) S. Ray, P. Das, A. Bhaumik, A. Dutta and C. Mukhopadhyay, *Appl. Catal., A*, 2013, **458**, 183–195; (*l*) L. Wang, X. Zhong, M. Zhou, W.-Y. Zhou, Q. Chen and M.-Y. He, *J. Chem. Res.*, 2013, **37**, 236–238; (*m*) V. Kannan and K. Sreekumar, *J. Mol. Catal. A: Chem.*, 2013, **376**, 34–39; (*n*) S. Laufer, D. Hauser, T. Stegmiller, C. Bracht, K. Ruff, V. Schattel, W. Albrecht and P. Koch, *Bioorg. Med. Chem. Lett.*, 2010, **20**, 6671–6675; (*o*) M. M. Heravi, F. Derikvand and F. F. Bamoharram, *J. Mol. Catal. A: Chem.*, 2007, **263**, 112–114.
31 K. M. Harmon and S. Pillar, *J. Mol. Struct.*, 2005, **740**, 75–80.
32 X. B. Wang, L. He, T. Y. Jian and S. Ye, *Chin. Chem. Lett.*, 2012, **23**, 13–16.
33 I. W. C. E. Arends and R. A. Sheldon, *Appl. Catal., A*, 2001, **212**, 175–187.